Single-mode InGaAs submonolayer quantum dot photonic crystal VCSELs

Single-mode InGaAs submonolayer quantum dot photonic crystal VCSELs

H P D Yang[1]**, I C Hsu**[2]**, F I Lai**[2]**, G Lin**[1]**, R S Hsiao**[1]**,
N A Maleev**[3]**, S A Blokhin**[3]**, H C Kuo**[2]**, S C Wang**[2]
and J Y Chi[1]

[1] Nanophotonic Center, Industrial Technology Research Institute, Chutung, Hsinchu 310,
Taiwan

[2] Institute of Electro-Optical Engineering, National Chiao Tung University,
1001 Ta Hsueh Road, Hsinchu 30050, Taiwan

[3] Ioffe Physico-Technical Institute, St Petersburg 194021, Russia

E-mail: hpyang@itri.org.tw

Abstract

An InGaAs submonolayer (SML) quantum dot photonic crystal
vertical-cavity surface-emitting laser (QD PhC-VCSEL) for fibre-optic
applications is demonstrated for the first time. The active region of the
device contains three InGaAs SML QD layers. Each of the InGaAs SML
QD layers is formed by alternate deposition of InAs (<1 ML) and GaAs.
Single-fundamental-mode CW output power of 3.8 mW at 28 mA has been
achieved in the 990 nm range, with a threshold current of 0.9 mA.
A side-mode suppression ratio (SMSR) larger than 35 dB has been observed
over the entire current operating range.

1. Introduction

Vertical-cavity surface-emitting lasers (VCSELs) have attracted a lot of attention in recent years. Single-mode VCSELs are necessary for a number of applications, including high-speed laser printing, optical storage and long-wavelength telecommunications. Small oxide aperture VCSELs below about 4 μm diameter operate in the fundamental transverse mode. However, the large resistance inherited from the small aperture limits the modulation bandwidth and degrades the high-speed performance. The lifetime of the oxide VCSEL also decreases proportionally to the diameter of the oxide aperture, even when the device is operated at a reduced current [1]. When the aperture diameter is increased to obtain higher output power, however, multiple higher order transverse modes oscillate, causing increased noise, a broadened spectrum and a strong increase of the far-field angle. Techniques used to solve the problem include the increase of higher order mode loss by surface-relief etching [2], hybrid oxide-implanted VCSELs [3, 4] and two-dimensional triangular holey structure [5]. Recently, a two-dimensional photonic crystal (2D PhC) structure formed on the VCSEL surface has been used as a control method of transverse modes. Single-mode output was realized from larger aperture photonic crystal VCSELs

(PhC-VCSELs) [6, 7]. However, those PhC-VCSELs exhibit relatively high threshold currents (I_{th}) due to large oxide-confined apertures. For long-wavelength applications, InAs quantum dot (QD) VCSELs [8] and QD PhC-VCSELs [9] achieved laser emission at 1300 nm. For shorter wavelength emission, InGaAs/GaAs submonolayer (SML) quantum dot (QD), embedded in a GaAs matrix shows luminescence peaks and high-power lasing performance in the 0.92–1 μm range [10]. Another approach is Stranski–Krastanow (SK) QDs, which contain InGaAs QD sheets separated by AlGaAs spacers [10]. Due to the better uniformity of the SML QDs, the SML QD laser surpasses the SK QD laser in output power characteristics. In this work, we choose SML QDs in our VCSEL structure, in order to achieve high-power performance.

Recently single-mode InGaAs SML QD VCSELs with room-temperature output power as high as 4 mW have been demonstrated [11]. However single-mode operation of the InGaAs SML QD VCSEL with PhC is still yet to be realized. In this paper, we report our results on the InGaAs QD PhC-VCSELs in the 990 nm range. Single-transverse-mode operation with a very high side-mode suppression ratio (SMSR) is demonstrated for the first time.
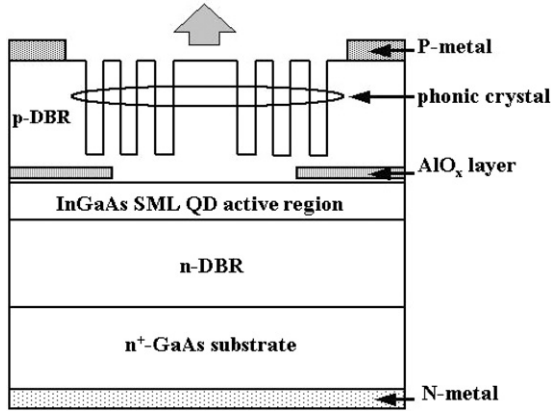
Figure 1. Schematic of InGaAs SML QD PhC-VCSEL. The hole etching depth of PhC is 16 pairs out of the 20-pair top DBR been etched off.
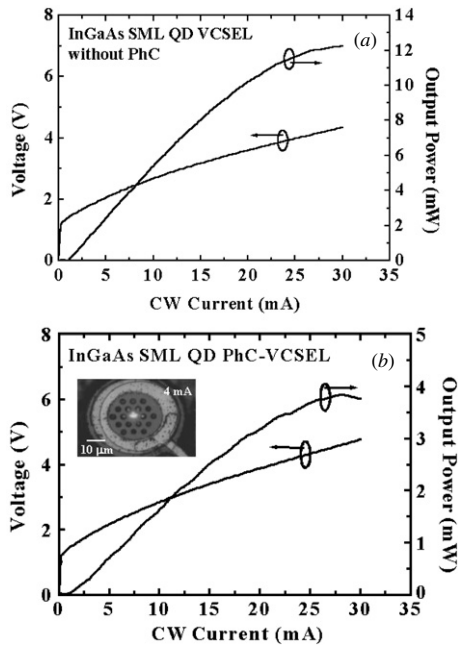

Figure 2. CW *L–I–V* characteristics and near-field image (inset) of an InGaAs SML QD VCSEL (*a*) without PhC and (*b*) with PhC, the ratio (α/Λ) is 0.5 and the lattice constant Λ is 5 μm.

Figure 3. Spectra of the InGaAs SML QD (*a*) PhC-VCSEL and (*b*) VCSEL without PhC holes, the ratio (α/Λ) is 0.5 and the lattice constant Λ is 5 μm.

Figure 4. Current-dependent lasing peak wavelength of the InGaAs SML QD PhC-VCSEL.

2. Experiment

The epitaxial layers of the InGaAs SML QD PhC-VCSEL wafers were grown on 3 inch n⁺-GaAs (0 0 1) substrates by molecular beam epitaxy (MBE) in Riber 49 chamber. The bottom distributed Bragg reflector (DBR) consists of a 33-pair n-type (Si-doped) quarter-wave stack ($\lambda/4$) of $Al_{0.9}Ga_{0.1}As$/GaAs. The top DBR consists of a 20-pair p-type (carbon-doped) $Al_{0.9}Ga_{0.1}As$/GaAs quarter-wave stack. Above that, is a heavily doped p-type GaAs contact layer. The undoped 1λ-cavity contains three InGaAs SML QD layers, separated by GaAs barrier layers. Each of the InGaAs SML QD layers is formed by alternate deposition of InAs (<1 ML) and GaAs. The current confinement of the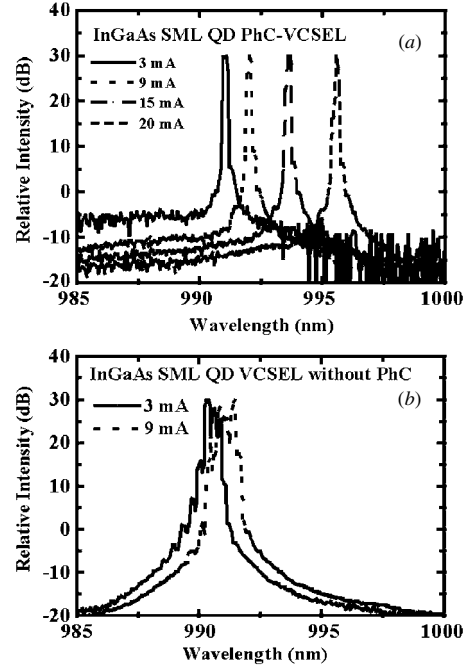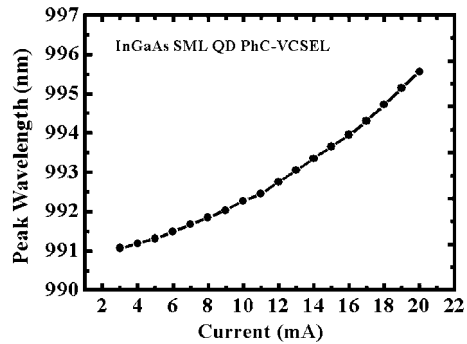 device was done by the selectively oxidized AlO_x tapered aperture. Firstly, mesas with diameters varying from 50 to 68 μm were defined by reactive ion etch (RIE). The p-contact ring with an inner diameter of 4 μm larger than the oxide aperture was formed on the top of the p-contact layer. The AlAs layer within the $Al_{0.9}Ga_{0.1}As$ confinement layers was selectively oxidized to AlO_x. The oxidation depth was about 16 to 17 μm towards the centre from the mesa edge so that the resulting oxide aperture varied from 16 to 36 μm in diameter. The oxide aperture was introduced at a minimum of the optical field in order to reduce the lateral optical loss and the leakage current. The n-contact was formed at the bottom of the n⁺-GaAs substrate. After that, triangular lattice patterns of photonic crystal with a single-point defect in the centre were defined within the p-contact ring using photolithography and were etched through the p-type DBR using RIE. The lateral index around a single defect can be controlled by the hole diameter (α)-to-lattice constant
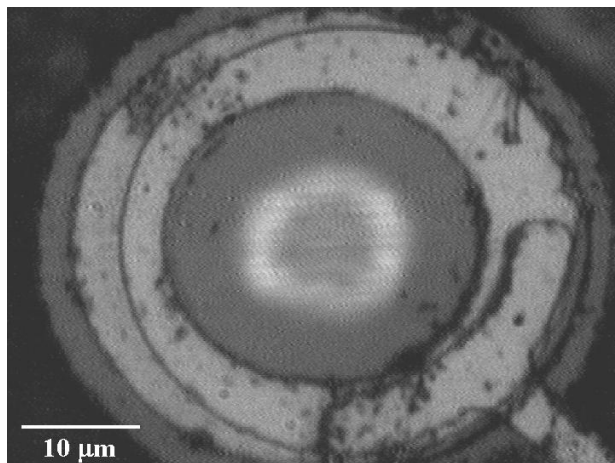
(*a*)
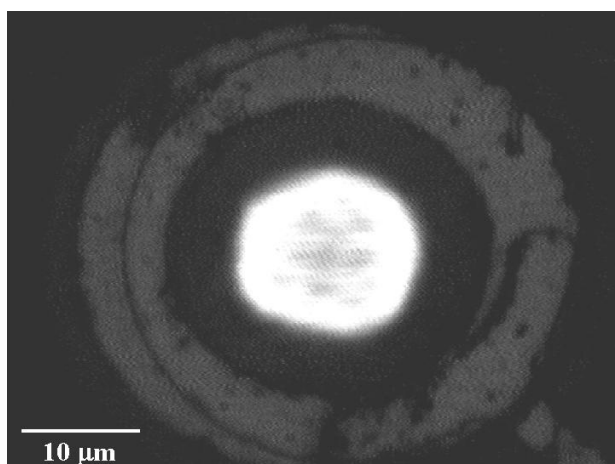
(*b*)
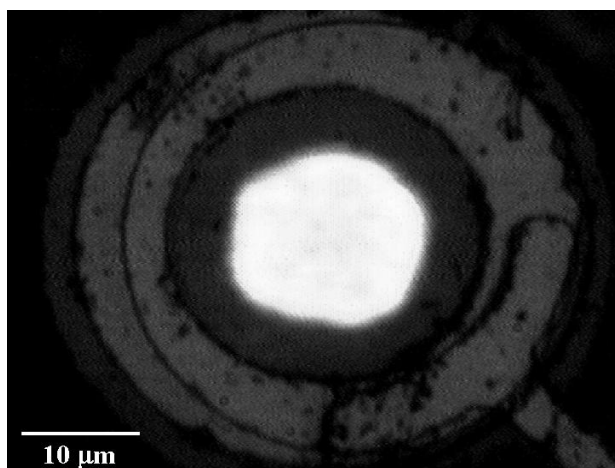
(*c*)

Figure 5. Near-field images of the InGaAs SML QD VCSEL without PhC at (*a*) 3 mA, (*b*) 9 mA and (*c*) 20 mA.

(Λ) ratio and etching depth [6]. This ratio (α/Λ) is 0.5; the lattice constant Λ is 5 μm in the PhC-VCSEL and the etching depth of the holes is about 16-pair thick into the 20-pair top DBR layer. The device structure is shown in figure 1. By using two types of apertures in this device, we decouple the effects
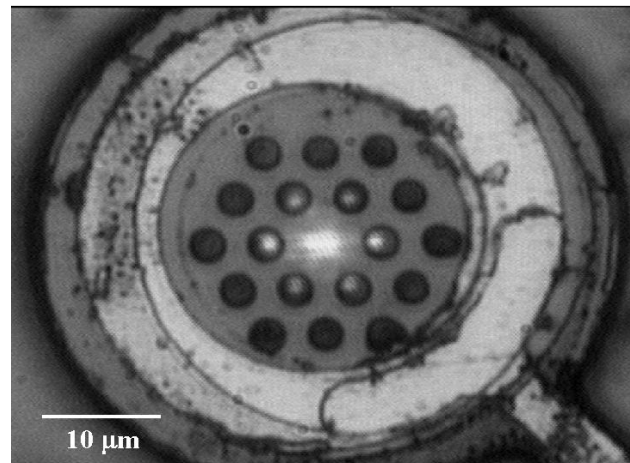
Figure 6. Near-field image of the InGaAs SML QD PhC-VCSEL at 10 mA.

of the current confinement from the optical confinement. The AlO$_x$ layer is used to confine the current flow, while the single-point defect (approximately $\geqslant 10$ μm in diameter) photonic crystal is used to confine the optical mode. In order to clarify the effect of the photonic crystal index-guiding layer, an oxide-confined VCSEL (oxide aperture = 16 to 18 μm in diameter without PhC) was also fabricated for comparison.

3. Results and discussion

Figure 2(*a*) shows the CW light–current–voltage (*L–I–V*) output of the InGaAs SML QD VCSEL without photonic crystal. The mesa of the VCSEL is 50 μm in diameter. The VCSEL shows a peak power of 12.2 mW at 30 mA, with a threshold current (I_{th}) of 1 mA. The differential series resistance is approximately 100 Ω at 12 mA. Figure 2(*b*) shows the CW *L–I–V* output of the PhC-VCSEL. The near-field image of the PhC-VCSEL operating at 4 mA is also shown (inset). The mesa of the VCSEL is also 50 μm. The PhC-VCSEL emits a maximum power of 3.8 mW at 28 mA and exhibits single-mode operation throughout the current range of operation. Near-field imaging of the output mode remains to be fundamental TEM$_{00}$ mode at the centre of the photonic crystal structure throughout the current operating range. I_{th} of the PhC-VCSEL is 0.9 mA. The differential series resistance of the PhC-VCSEL is approximately 125 Ω at 12 mA. The *I–V* characteristics exhibit slightly higher series resistance for the PhC-VCSEL, which would be mainly due to blocking of the current flow in the region by photonic crystal holes. Lasing spectra of the PhC-VCSEL are shown in figure 3(*a*), confirming single-mode operation within the overall operation current. The peak lasing wavelengths are 991, 992, 994 and 996 nm at 3 mA, 9 mA, 15 mA and 20 mA, respectively. The PhC-VCSEL exhibits an SMSR >35 dB throughout the current range. The peak wavelength versus injection current plot of the InGaAs SML QD PhC-VCSEL is shown in figure 4. The peak lasing wavelength increases monotonically with increasing injection current. The increase in wavelength with increasing injection current is mainly due to increasing junction temperature. The lasing in QDs is believed to be
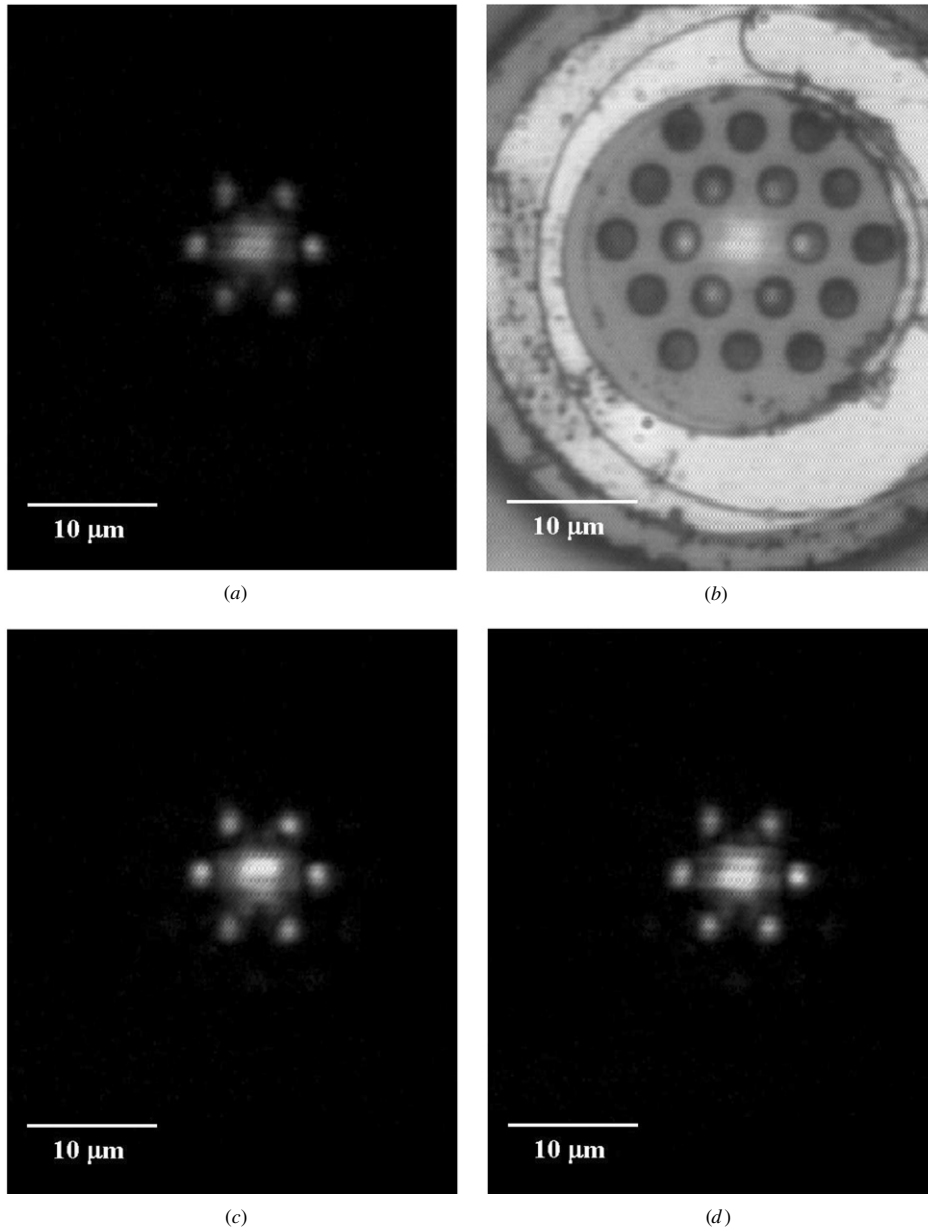
Figure 7. Near-field images of the InGaAs SML QD PhC-VCSEL at (*a*) 8 mA, (*b*) 10 mA, (*c*) 16 mA and (*d*) 20 mA.

ground-state transition since all the measured spectra are single mode for the PhC-VCSELs. No side mode corresponding to an excited state transition was observed at higher currents. For comparison, lasing spectra of the InGaAs QD VCSEL without photonic crystal holes show multiple mode operation as the driving current is increased above I_{th} (figure 3(*b*)). The InGaAs SML QD VCSEL without PhC shows multiple transverse mode characteristics with a broader wavelength span. The near-field images of the VCSEL without PhC are shown in figure 5. The near-field image of the VCSEL at 3 mA (figure 5(*a*)) was taken with light illumination to show the relative position of the lasing area with respect to the p-contact ring. The lasing area is annular in shape with lower intensity in the central region. The near-field images at 9 mA and 20 mA (figures 5(*b*) and (*c*)) show lasing areas with higher intensity at the centre. The lasing area of the device at 20 mA

is about 16 μm in diameter, which is close to the diameter of the oxide aperture. All the near-field images show that the laser beam is of multimode characteristics because of the larger oxide aperture (approximately 16 to 18 μm in diameter) of the device. With the same oxide aperture size, the VCSELs with a PhC structure clearly show much better optical confinement. Figure 6 shows the near-field image of the PhC-VCSEL at 10 mA. The laser output is a fundamental TEM_{00} mode at the centre of the PhC structure. The TEM_{00} mode is round in shape with a diameter of approximately 4.3 μm. Smaller lasing spots emitting from the nearby photonic crystal holes with lower intensity were also observed. These lasing spots are mainly the scattered and diffracted laser beams from the TEM_{00} beam at the centre, which are all emitting with the same lasing wavelength. The near-field images of the PhC-VCSEL at different current levels are shown in figure 7. We observed

continuous changes in the near-field image of the PhC-VCSEL. The lasing area consists of the fundamental TEM$_{00}$ mode at the centre and six smaller lasing spots surrounding it. The intensity of all the lasing spots, including the TEM$_{00}$ mode at the centre, increases with increasing current. The near-field image at 10 mA was taken with light illumination in order to show the relative position of the lasing spots with respect to the photonic crystal structure simultaneously. These six smaller lasing spots are found to be emitting out of the six photonic crystal holes near the centre. These lasing spots are the scattered and diffracted laser beams contributed from the TEM$_{00}$ mode at the centre, which transmit the photonic crystal holes easily because of the lower reflectivity of the remaining DBR layers under these holes. The etching depth of the photonic crystal hole is 16 pairs into the 20-pair top DBR. The reflectivity under the photonic crystal hole area is lowered from approximately 99% of the top DBR to about 30 to 40% after etching. These lasing spots can also be observed by the near-field imaging because of the very high overall output power of the InGaAs SML QD PhC-VCSEL.

4. Conclusion

We have demonstrated a high-power, single-mode InGaAs SML QD PhC-VCSEL with SMSR >35 dB throughout the current operating range. The maximum output power is 3.8 mW, which is the highest reported for the PhC-VCSELs. The present results indicate that a VCSEL using an oxide layer for current confinement and photonic crystal for optical confinement is a promising approach to achieve single-mode operation of VCSELs.

References

[1] Hawkins B M, Hawthorne R A III, Guenter J K, Tatum J A and Biard J R 2002 *Proc. 52nd Electron. Comp. & Technol. Conf.* pp 540–50
[2] Haglund A, Gustavsson J S, Vukusic J, Modh P and Larsson A 2004 *IEEE Photonics Technol. Lett.* **16** 368–70
[3] Hsueh T H, Kuo H C, Lai F I, Laih L H and Wang S C 2003 *Electron. Lett.* **39** 1519–21
[4] Young E W, Choquette K D, Chuang S L, Geib K M, Fischer A J and Allerman A A 2001 *IEEE Photonics Technol. Lett.* **13** 927–9
[5] Furukawa A, Sasaki S, Hoshi M, Matsuzono A, Moritoh K and Baba T 2004 *Appl. Phys. Lett.* **85** 5161–4
[6] Yokouchi N, Danner A J and Choquette K D 2003 *Appl. Phys. Lett.* **82** 1344–6
[7] Berkedal D, Gregersen N, Bischoff S, Madsen M, Romsted F and Oestergarrd J 2003 *Proc. Optical Fiber Comm. Conf.* pp 83–5
[8] Lott J A, Ledentsov N N, Ustinov V M, Maleev N A, Zhukov A E, Kovsh A R, Maximov M V, Volvovik B V, Alferov Z H I and Bimberg D 2000 *Electron. Lett.* **36** 1384–5
[9] Yang H P D, Chang Y H, Lai F I, Yu H C, Hsu Y J, Lin G, Hsiao R S, Kuo H C, Wang S C and Chi J Y 2005 *Electron. Lett.* **41** 1130–2
[10] Mikhrin S S *et al* 2000 *Semicond. Sci. Technol.* **15** 1061–4
[11] Blokhin S A *et al* 2006 *Semiconductors* **40** 663–8